J. Fluid Mech. (1973), *vol.* 57, *part* 1, *pp.* 45–61
Printed in Great Britain

Transpiration and natural convection: the vertical-flat-plate problem

By J. F. CLARKE
Department of Aerodynamics, Cranfield Institute of Technology, Bedford.

(Received 30 June 1972)

A study is made of the natural convective flow which is induced in an infinite expanse of gas by the presence of a vertical hot flat plate from which hot gas of the same chemical type is being blown. The transpiration rate is assumed to be such that a self-similar boundary-layer type of solution is available. It differs from previous analyses in the following respects. Most important, the density is not assumed to be constant at any stage in the description of the flow field. Also the form of the induced flow in the outer domain is calculated and proves to be substantially independent of the blowing rate in this case; the induced outer flow is found to be of large lateral extent. Finally, the variable-gas-property problem is carried to second order and solutions are obtained by using an 'exact' form of Howarth–Dorodnitsyn variable. The opportunity is taken to make some comments about the comparison between theory and experiment for finite flat plates without transpiration.

1. Introduction

Previous solutions of the effects of mass transfer on the natural convective motion past a heated vertical flat plate have been given by Eichhorn (1960) and Sparrow & Cess (1961). Eichhorn examined similarity solutions in the context of a boundary-layer theory (essentially the large-Grashof-number case) while Sparrow & Cess gave an approximate boundary-layer analysis for the non-self-similar situation which arises when both the plate temperature and transpiration rate are constant. The latter problem has very recently (while the current work was being written up, in fact) been taken up again by Merkin (1972). All these writers make the assumption that the density of the convected material is constant everywhere except in the momentum-equation forcing term which drives the natural convective motion, and additionally confine themselves to the first-order boundary-layer approximation.

When temperature variations in a gas are of substantial amplitude the constant-density approximation is poor, and it is a prime purpose of the present article to retain the density variations in full. Note too that attention is here confined to transpired and ambient gases of the same chemical type. Furthermore, it is intended to proceed to a higher level of approximation in large-Grashof-number theory and in this way to investigate the slow flow which is induced in the outer, inviscid, constant-temperature domain, as well as the important effects which

this outer flow itself induces in the inner, boundary-layer-like, region. The opportunity is taken to make come comments about the present second-order results for a semi-infinite flat plate and the available theoretical and experimental results for the impermeable finite chord surface.

The original motivation for the present work was a desire to know something about the interaction between combustion and natural convection, where density and temperature variations will undoubtedly be very large. The transpired gas in such a case reacts chemically with the external atmosphere and it is hoped to report progress on this more complex problem at a later date.

2. Conservation equations

With the assumptions of constant specific heat and low Mach number (e.g. $< 10^{-2}$) the set of conservation and thermodynamic equations for a steady two-dimensional natural-convective system takes the form

$$\frac{\partial}{\partial x}(\rho u)+\frac{\partial}{\partial z}(\rho w) = 0, \tag{1}$$

$$\rho u\frac{\partial u}{\partial x}+\rho w\frac{\partial u}{\partial z}+\frac{\partial p}{\partial x} = 1-\rho+\epsilon\left\{\frac{\partial}{\partial x}\left[\tfrac{4}{3}\mu\frac{\partial u}{\partial x}-\tfrac{2}{3}\mu\frac{\partial w}{\partial z}\right]+\frac{\partial}{\partial z}\left[\mu\frac{\partial u}{\partial z}+\mu\frac{\partial w}{\partial x}\right]\right\}, \tag{2}$$

$$\rho u\frac{\partial w}{\partial x}+\rho w\frac{\partial w}{\partial z}+\frac{\partial \rho}{\partial z} = \epsilon\left\{\frac{\partial}{\partial x}\left[\mu\frac{\partial w}{\partial x}+\mu\frac{\partial u}{\partial z}\right]+\frac{\partial}{\partial z}\left[\tfrac{4}{3}\mu\frac{\partial w}{\partial z}-\tfrac{2}{3}\mu\frac{\partial u}{\partial x}\right]\right\}, \tag{3}$$

$$\rho u\frac{\partial \theta}{\partial x}+\rho w\frac{\partial \theta}{\partial z} = \frac{\epsilon}{Pr}\left\{\frac{\partial}{\partial x}\left(\lambda\frac{\partial \theta}{\partial x}\right)+\frac{\partial}{\partial z}\left(\lambda\frac{\partial \theta}{\partial z}\right)\right\}, \tag{4}$$

$$\rho\theta = 1. \tag{5}$$

The variables in this set of equations are all dimensionless, as follows: the gravitational acceleration g is directed along the negative-x axis and, together with some suitable length scale L, makes up a typical speed U such that

$$U = (gL)^{\frac{1}{2}}; \tag{6}$$

the velocity components u and w, directed along the x and z axes respectively, are measured in units of U, while x and z themselves are measured in units of L; the dimensional density is found by multiplying the no-flow density ρ_0 (assumed constant) by the number ρ; the *flow-induced* pressure changes are given by $\rho_0 U^2 p$ and the absolute temperature is equal to $T_0\theta$, where T_0 is the constant no-flow temperature; μ and λ are the dynamic viscosity and thermal conductivity measured in units of the constants μ_0 and λ_0, which are the no-flow viscosity and conductivity, respectively; Pr is the usual Prandtl number and ϵ is the reciprocal square-root of the Grashof number, i.e.

$$\epsilon = (Gr)^{-\frac{1}{2}}, \quad Gr = \rho_0^2 L^3 g/\mu_0^2. \tag{7}$$

Generally speaking the Grashof number is large and it is with this case that we are exclusively concerned here.

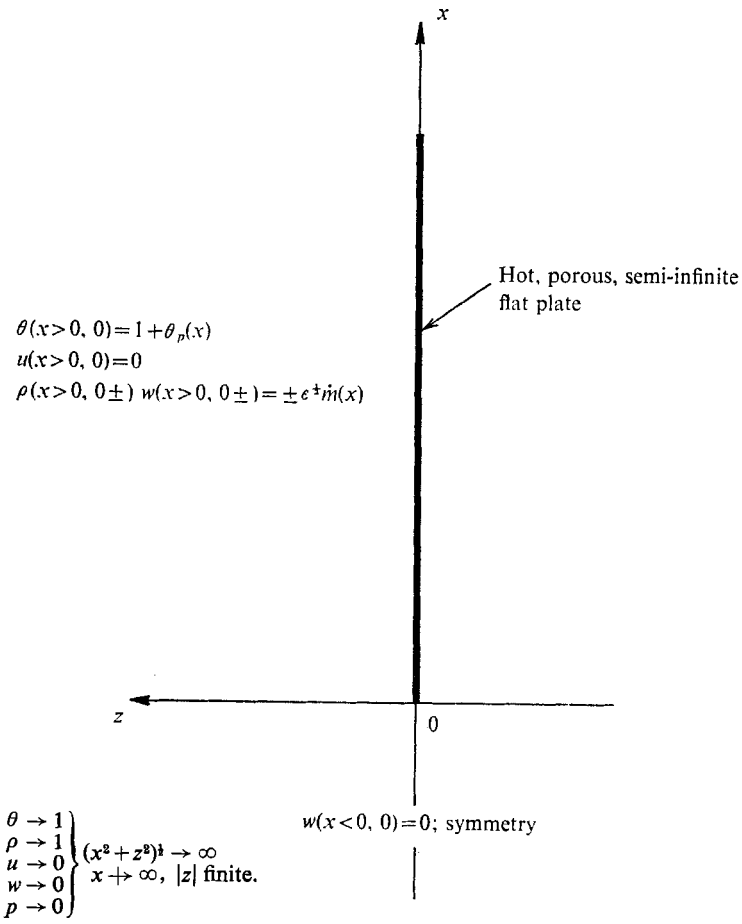

FIGURE 1. Geometric arrangement and boundary values.

Figure 1 is a sketch of the geometric arrangement and also exhibits the requisite boundary-value information. It is advantageous to introduce a stream function ψ which is defined so that

$$\rho u = \partial\psi/\partial z, \quad \rho w = -\partial\psi/\partial x, \tag{8}$$

and which thereby ensures that (1) is satisfied.

3. Outer solutions: first estimates

It is possible to identify an outer domain D_0 (namely $|z| \neq 0$, all x) in which the outer limit ($\epsilon \to 0$; x, z fixed) operates and within which the dependent variables have asymptotic representations

$$f(x, z: \epsilon) = \sum_{n=1}^{N} g_f^{(n)}(\epsilon) f^{(n)}(x, z) + o(g_f^{(N)}), \tag{9}$$

where f is equal to ρ, θ, u, w, ψ or p, as is appropriate.

The first outer solutions are as follows:

$$g_\theta^{(1)}(\epsilon) = 1, \quad \theta^{(1)}(x,z) = 1; \tag{10}$$

$$g_\rho^{(1)}(\epsilon) = 1, \quad p^{(1)}(x,z) = 1; \tag{11}$$

$$g_f^{(1)}(\epsilon) = o(1), \quad f = u, w, \psi \text{ or } p. \tag{12}$$

No values for the first significant gauge or coefficient functions for u, w, ψ or p can be found until the non-uniformities which exist as a result of the failure of θ to meet the boundary conditions on θ and w have been resolved.

4. Inner solutions: first terms

The inner domain D_i is $x > 0$ with $|z| \to 0$ as $\epsilon \to 0$; with the inner co-ordinates x and Z, the latter being defined so that

$$Z = z\epsilon^{-\frac{1}{2}}, \tag{13}$$

application of the inner limit ($\epsilon \to 0$, x and Z fixed) permits construction of inner asymptotic series

$$f(x,z:\epsilon) = \sum_{n=1}^{M} G_f^{(n)}(\epsilon)\,\mathscr{F}^{(n)}(x,Z) + o(G_f^{(M)}), \tag{14}$$

where the function $\mathscr{F}$ is Θ, R, U, W, Ψ or P when f is θ, ρ, u, w, ψ or p, respectively. It readily follows that the first inner gauge functions which permit matching with the outer solutions are

$$G_f^{(1)}(\epsilon) = 1, \quad f = \theta, \rho, u; \quad G_f^{(1)}(\epsilon) = \epsilon^{\frac{1}{2}}, \quad f = w, \psi; \quad G_f^{(1)}(\epsilon) = o(1), \quad f = p. \tag{15}$$

The coefficient functions $\mathscr{F}^{(1)}$ for the case of a plate of constant temperature,

$$\theta_p(x) = \Delta, \tag{16}$$

are found from the similitudes

$$\Psi^{(1)}(x,Z) = C^{\frac{1}{2}}\Delta^{\frac{1}{4}}(4x)^{\frac{3}{4}}F(\eta), \tag{17}$$

$$\Theta^{(1)}(x,Z) = 1 + \Delta H(\eta), \tag{18}$$

where

$$\eta = \Delta^{\frac{1}{4}}Y/C^{\frac{1}{2}}(4x)^{\frac{1}{4}}, \tag{19}$$

$$Y = \int_0^Z R^{(1)}(x,s)\,ds, \tag{20}$$

and C is the Chapman–Rubesin factor (i.e. a mean constant value of the product $\rho\mu$; if the viscosity and thermal conductivity are proportional to temperature, C is equal to unity). The reduced stream function F and reduced temperature H satisfy the pair of simultaneous nonlinear ordinary differential equations

$$F''' + 3FF'' - 2F'^2 + H = 0, \tag{21}$$

$$H'' + 3PrFH = 0, \tag{22}$$

where a prime denotes differentiation with respect to the similarity variable η.

The boundary condition satisfied by H is evidently

$$H(0) = 1 \tag{23}$$

and matching of solutions in the overlap region of D_0 and D_i leads to the requirement

$$H(\eta \to \infty) \to 0. \tag{24}$$

The x component of the velocity in D_i can be found, with the aid of (8), (14), (15), (17), (19) and (20), from the result

$$U^{(1)} = (\partial \Psi^{(1)}/\partial Y)_x = (4\Delta x)^{\frac{1}{2}} F'(\eta),$$

so that the no-slip condition makes

$$F'(0) = 0. \tag{25}$$

To a first approximation the value of ρw in D_i is given by

$$\rho w \sim -\epsilon^{\frac{1}{2}} \left(\frac{\partial \Psi^{(1)}}{\partial x}\right)_Z = -\epsilon^{\frac{1}{2}} \left\{\left(\frac{\partial \Psi^{(1)}}{\partial x}\right)_Y + \left(\frac{\partial \Psi^{(1)}}{\partial Y}\right)_x \left(\frac{\partial Y}{\partial x}\right)_Z\right\}. \tag{26}$$

When z, Z and Y all approach zero the final term in (26) vanishes and so the boundary condition on ρw as $z \downarrow 0$ makes

$$\dot{m}(x) = -[\partial \Psi^{(1)}(x, 0)/\partial x]_Y.$$

However, (17) shows that

$$(\partial \Psi^{(1)}/\partial x)_Y = C^{\frac{1}{2}} (\Delta/4x)^{\frac{1}{4}} \{3F(\eta) - \eta F'(\eta)\},$$

whence it follows that

$$\dot{m}(x) = -3C^{\frac{1}{2}} (\Delta/4x)^{\frac{1}{4}} F(0). \tag{27}$$

If the similitude expressed in (17)–(20) is to be preserved, (27) shows that $\dot{m}(x)$ must be proportional to $x^{-\frac{1}{4}}$; choosing

$$\dot{m}(x) = C^{\frac{1}{2}} (\Delta/4x)^{\frac{1}{4}} M, \tag{28}$$

where M is a 'mass-flux' constant, (27) and (28) show that the boundary condition for F is

$$3F(0) = -M. \tag{29}$$

Matching the u component of velocity yields the final condition,

$$F'(\eta \to \infty) \to 0, \tag{30}$$

and completes the specification of the first inner problem. When M is zero this reduces to the classical natural convection problem, for a detailed discussion of which one may consult the work of Ostrach (1964) or the subsequent review by Ede (1967); present attention will be confined to the case $M \geqslant 0$.

It can be shown by elementary reasoning that any solutions of 21 and 22 which satisfy conditions (23), (24), (25), (29) and (30) must be such that $H(\eta)$ and $F'(\eta)$ approach zero exponentially in the limit as η grows without bound; also F must tend to a positive *finite limit* $F(\infty)$ with $F(\infty) - F(\eta \to \infty)$ approaching zero exponentially.

5. Numerical inner solutions

Solution of the problem presented by (21) and (22) is complicated by the two-point boundary conditions, which make it necessary to guess both $F''(0)$ and

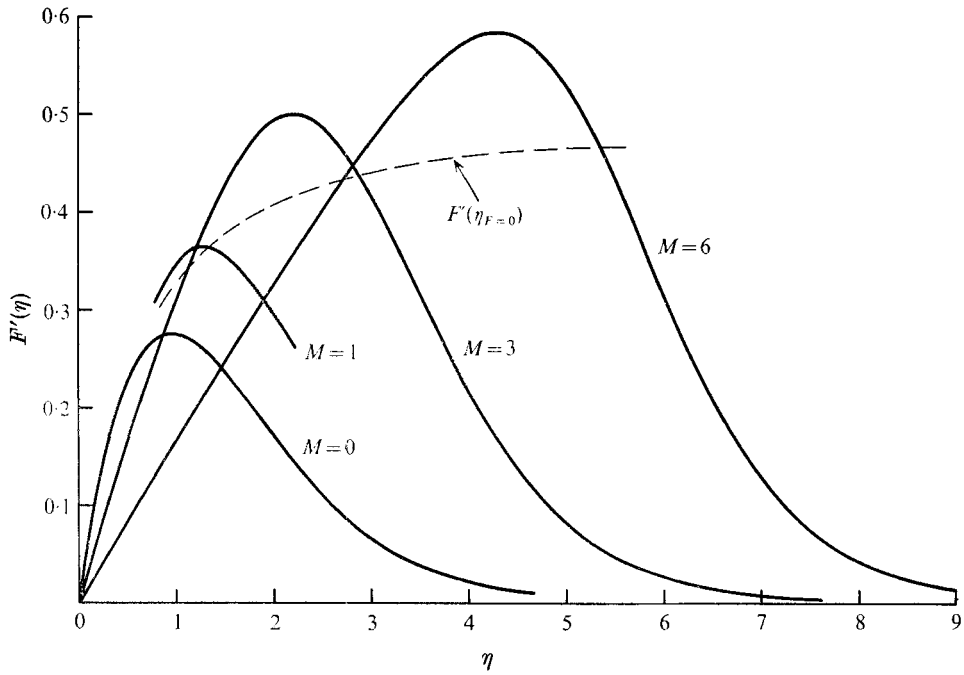

FIGURE 2. The velocity function $F'(\eta)$ [see equation (25)] versus η [see equation (19)] for various values of the blowing constant M [see equation (28)]. $F'(\eta_{F=0})$ is the locus of F' on the dividing streamline.

$H'(0)$ in such a way as to satisfy (24) and (30); the fact that the last pair of conditions are to apply in the limit as $\eta \to \infty$ is an additional complicating factor. Two distinct techniques have been applied in order to arrive at the desired solutions: the first takes note of the existing solution for $M = 0$ and uses the method of parametric differentiation (described by Ruppert & Landahl 1967) to extend this into the domain $M > 0$; the second technique, due to Nachstheim & Swigert (1965), adjusts the initial guesses for $F''(0)$ and $H'(0)$ so that a sum of the mean-square errors between the computed variables and the asymptotic values is minimized. The first method makes heavy demands on computer space as a result of its requirement of full details of the behaviour of F, F', etc. for some initial value of M; the second method, being basically iterative, occupies more computing time for a given M value than the first method. In the range of values of M for which the methods have been compared (namely $0 \leqslant M \leqslant 3$) there is no significant disagreement of predictions at the lower end of the range; at the larger values of M discrepancies between results from the two methods do occur and, even though these are not of a radical kind, the Nachtsheim & Swigert least-square-error technique is to be preferred; the latter procedure has been used to carry the computations as far as $M = 8$ in steps of 0·5. Some typical results for $F'(\eta)$ and $H(\eta)$ are given in figures 2 and 3 and tables 1 and 2. There is substantial agreement with the functions calculated by Eichhorn (for example, the curves for $M = 3$ are indistinguishable on the scale of the figures; no table of values of F' and H is given by Eichhorn) but the present results go somewhat further and

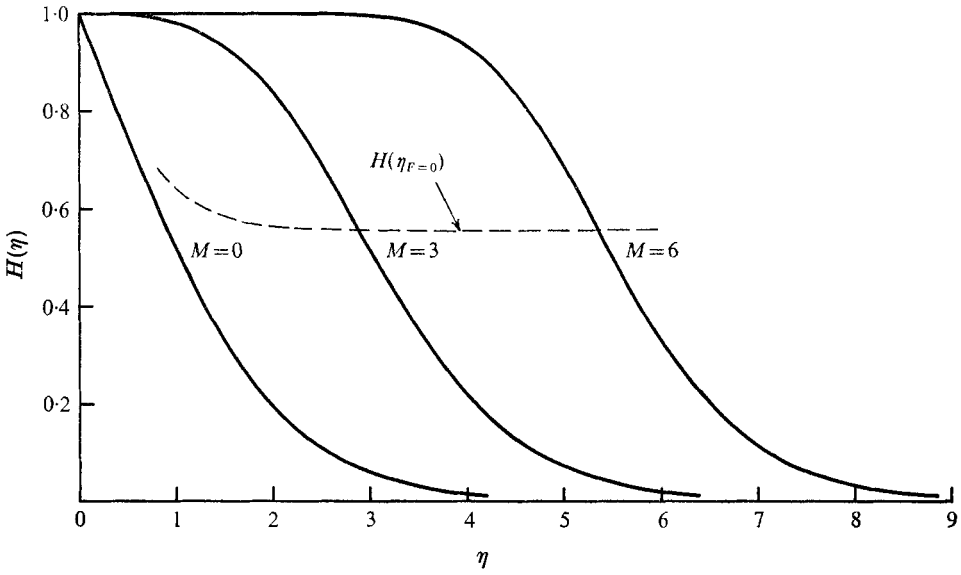

FIGURE 3. Dimensionless temperature difference $H(\eta)$ versus η for various values of the blowing constant. $H(\eta_{F=0})$ is the value of H on the dividing streamline.

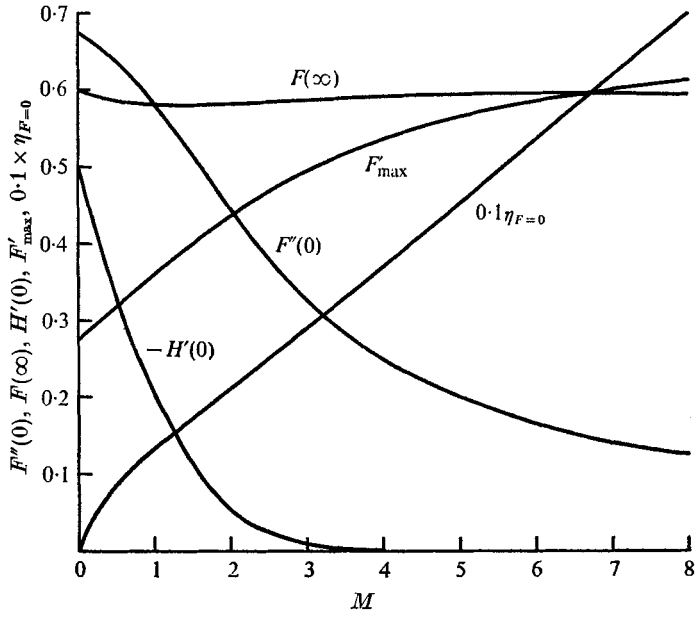

FIGURE 4. Dependence of skin friction $F''(0)$, asymptotic stream function $F(\infty)$, heat-transfer rate $H'(0)$, maximum velocity F'_{max} and dividing streamline location $\eta_{F=0}$ on the value of the blowing constant.

	$F'(\eta)$		
η	$M = 0$	$M = 3$	$M = 6$
0	0	0	0
0·4	0·1962	0·1283	0·0665
0·8	0·2708	0·2489	0·1326
1·2	0·2668	0·3553	0·1979
1·6	0·2238	0·4382	0·2622
2·0	0·1699	0·4863	0·3250
2·4	0·1207	0·4909	0·3859
2·8	0·0818	0·4527	0·4442
3·2	0·0537	0·3833	0·4916
3·6	0·0344	0·3010	0·5444
4·0	0·0216	0·2220	0·5763
4·4	0·0134	0·1558	0·5838
4·8	0·0083	0·1053	0·5576
5·2	0·0051	0·0691	0·4965
6·0	0·0018	0·0282	0·3167
6·8	0·0007	0·0109	0·1595
7·6	0·0002	0·0041	0·0693
8·4	0·0001	0·0015	0·0277
9·2	0·0000	0·0005	0·0105
10·0	0·0000	0·0002	0·0039

TABLE 1

	$H(\eta)$		
η	$M = 0$	$M = 3$	$M = 6$
0	1	1	1
0·4	0·7988	0·9952	1
0·8	0·6059	0·9843	1
1·2	0·4350	0·9606	1
1·6	0·2969	0·9148	1
2·0	0·1945	0·8373	0·9998
2·4	0·1235	0·7255	0·9993
2·8	0·0767	0·5889	0·9974
3·2	0·0469	0·4470	0·9912
3·6	0·0284	0·3189	0·9744
4·0	0·0171	0·2163	0·9362
4·4	0·0103	0·1412	0·8646
4·8	0·0061	0·0896	0·7543
5·2	0·0037	0·0558	0·6145
6·0	0·0013	0·0210	0·3317
6·8	0·0005	0·0077	0·1451
7·6	0·0002	0·0028	0·0566
8·4	0·0000	0·0010	0·0210
9·2	0·0000	0·0003	0·0076
10·0	0·0000	0·0001	0·0027

TABLE 2

deal, too, with larger values of M. Figure 4 illustrates results for a number of interesting special values. From the definitions of ψ in (8), Z in (13) and various results in (15)–(20) it follows that

$$U^{(1)} = \Psi_Y^{(1)} = (4\Delta x)^{\frac{1}{2}} F'(\eta), \tag{31}$$

$$\left.\frac{\partial U^{(1)}}{\partial Z}\right|_{Z=0} = \frac{(4x)^{\frac{1}{4}}\Delta^{\frac{3}{4}}}{(1+\Delta)\sqrt{C}} F''(0), \tag{32}$$

$$\left.\frac{\partial \Theta^{(1)}}{\partial Z}\right|_{Z=0} = \frac{\Delta^{\frac{5}{4}}}{(1+\Delta)(4x)^{\frac{1}{4}}\sqrt{C}} H'(0). \tag{33}$$

Thus, referring again to figure 4, $F'_{\max}$ indicates how the maximum velocity parallel to the plate at a fixed x increases with increasing mass flux through the plate. Equation (32) shows that $F''(0)$ is proportional to the skin friction at the plate and figure 4 shows that, even though it does diminish with increasing transpiration rate, the skin friction is still far from zero, even at $M = 8$. It would appear to be quite difficult to 'blow off' the present natural-convective shear layer. Equation (33) shows that $H'(0)$ is proportional to the rate of heat conduction at the solid surface, which, since $H'(0) < 0$, is *from* the plate *to* the gas in all circumstances. Figure 4 makes it very clear that this heat-conduction rate diminishes dramatically with increased transpiration rate; at an M of 3·5, $H'(0)$ has the value $2{\cdot}11 \times 10^{-3}$ and this has fallen to $2{\cdot}441 \times 10^{-11}$ when M is equal to 8. The wide (in terms of η) region of gas at a nearly constant temperature which occurs at the higher transpiration rates is evident from figure 3.

The gas which is injected through the surface of the plate is all convected into the space between the plate and the line which is the locus of $F(\eta)$ equal to zero; the value of η which makes F vanish is defined to be $\eta_{F=0}$ and its variation with M is indicated in figure 4. The shape of the dividing streamline in the inner domain which separates transpired gas from the gas which is convected naturally from the exterior regions is therefore given by (19) in the form

$$Y = C^{\frac{1}{2}}\Delta^{-\frac{1}{4}}(4x)^{\frac{1}{4}}\eta_{F=0}, \tag{34}$$

and one must remember that Y itself is a function of Z and x through (20). It is convenient hereafter to refer to the flow in $0 \leqslant \eta < \eta_{F=0}$ as the interior flow and to that in $\eta_{F=0} < \eta$ as the exterior flow. It is observed from (22) that $\eta_{F=0}$ is the location of the inflexion point in the $H(\eta)$ curves.

The value to which F tends in the limit as $\eta \to \infty$, namely $F(\infty)$, is indicative of the mass of gas which, up to any given x location, is entrained from the exterior regions of the flow field by the natural convective processes [see equation (17)]. Figure 4 shows the interesting fact that $F(\infty)$ is practically independent of the transpiration rate in this constant-plate-temperature, self-similar configuration. The establishment of a mass flux of gas is encouraged by heating of the fluid and inhibited by the no-slip condition at the plate. When transpiration takes place the exterior flow (in the sense defined in the previous paragraph) finds itself in a state of relatively low temperature, as one can see by consulting figure 4, but it is at the same time removed from the constraint of no slip and is actually being dragged upwards by the interior flow at the higher values of M. These two

contrary influences seem to conspire in the present instance to cancel one another out. From the portion of the curve of $F'(\eta)$ at an M of unity which is sketched in figure 2 it is clear that $F'_{\max}$ and $F'(\eta_{F=0})$ coincide for an M value slightly less than one. For smaller M values the inner flow actually exerts a small restraining shear stress on the outer flow; this fact combined with the reduced temperatures in the outer flow for all M values (consult the locus $H(\eta_{F=0})$ on figure 3) is responsible for the slight initial reductions in $F(\infty)$ as M increases from zero.

6. Completion of the first outer solutions

With the information available from the first inner solutions it is now possible to evaluate those components of the first significant outer solutions which have $o(1)$ gauge factors [see equation (12)]. In particular, matching of the stream functions shows that

$$g_{\psi}^{(1)}(\epsilon) = \epsilon^{\frac{1}{2}}; \quad \psi^{(1)}(x > 0, 0) = C^{\frac{1}{2}}\Delta^{\frac{1}{4}}(4x)^{\frac{3}{4}}F(\infty). \tag{35}$$

The value of the temperature in D_i is $1+\Delta H(\eta)$ to first order; since $H(\eta)\to 0$ like $\exp(-\text{constant}\times\eta)$ as $\eta\to\infty$ it follows from matching that $g_{\theta}^{(n)}(\epsilon)$ is $o(\epsilon^{\frac{1}{2}n})$ for all $n \geqslant 2$, with a similar conclusion for $g_{\rho}^{(n)}(\epsilon)$ following from (5). It is inferred, ignoring exponentially small terms, that $\theta = 1 = \rho$ in D_i and the outer flow, which is induced by the presence of the natural convective boundary layer in D_o, is of the constant-temperature incompressible type. It can now be deduced that

$$g_u^{(1)}(\epsilon) = \epsilon^{\frac{1}{2}} = g_w^{(1)}(\epsilon); \quad g_p^{(1)}(\epsilon) = \epsilon, \tag{36}$$

and also that the flow in D_o is irrotational.

Solutions for the complex-conjugate velocity, $u^{(1)}-iw^{(1)}$, which satisfy the condition in (35) supplemented by the symmetry requirement

$$\psi^{(1)}(x < 0, 0) = 0, \tag{37}$$

can be obtained by the usual complex-variable methods, and this has been done by Yang & Jerger (1964) for the no-blowing case, $M = 0$. (In fact Yang & Jerger were primarily interested in the finite and not the semi-infinite flat plate, but solutions for the latter problem appear as a special case of their analysis; the work of Yang & Jerger will be referred to again in the next section in another context.) The fact that $F(\infty)$ varies so little for $M \geqslant 0$ means that not only the form of $u^{(1)}-iw^{(1)}$ but also its magnitude is effectively unaltered, whether blowing takes place or not.

A picture of the flow induced in D_o by the presence of the hot semi-infinite plate and the hot transpired gas is provided by sketching one or two streamlines from the solution for $\psi^{(1)}$ (which incidentally is *not* given by Yang & Jerger). It easily follows that

$$\psi^{(1)} = \tfrac{4}{3}A(x^2+z^2)^{\frac{3}{8}}\sin\{\tfrac{3}{4}\tan^{-1}(z/x)+\tfrac{1}{4}\pi\}, \tag{38}$$

where

$$A \equiv 3C^{\frac{1}{2}}\Delta^{\frac{1}{4}}F(\infty), \tag{39}$$

and figure 5 illustrates the results, with the gas speed written as q, where

$$q \equiv \epsilon^{\frac{1}{2}}[u^{(1)2}+w^{(1)2}]^{\frac{1}{2}} = \epsilon^{\frac{1}{2}}A(x^2+z^2)^{-\frac{1}{8}}, \tag{40}$$

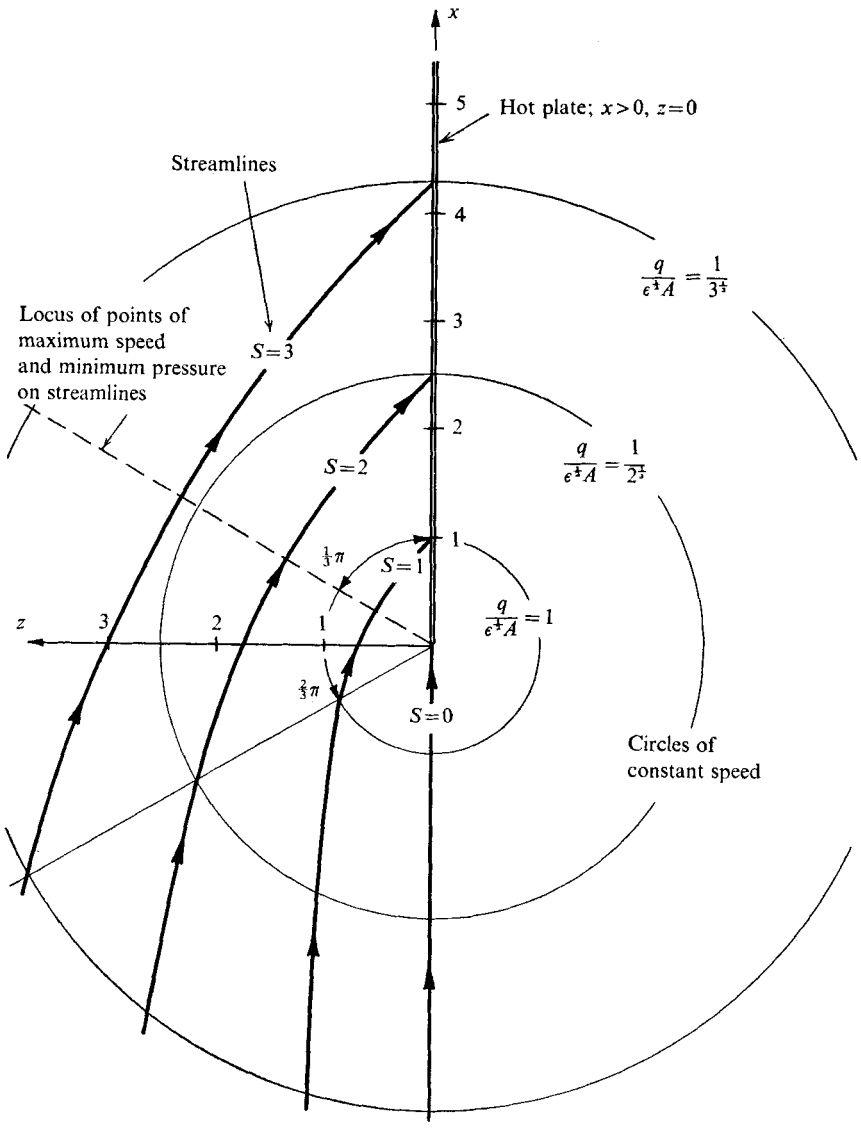

FIGURE 5. Streamlines of the induced outer-domain flow.

the streamline number S being defined as

$$S = 3(2^{\frac{1}{2}})\psi^{(1)}/4A. \tag{41}$$

Attention is drawn particularly to the existence of a maximum speed and hence minimum pressure on any streamline (the locus of such points is indicated on the figure) and also to the large lateral extent of the 'catchment area' for material which finds its way into the boundary layer in D_1. When viewed from D_0 the appearance of the plate as a line of sinks is clear, as is the fact that this sink-like property of the plate induces a positive slip velocity along the solid surface. It is worth reiterating that the situation illustrated in figure 5, namely a

view of the flow from the domain D_0, is the same whether transpiration through the plate is taking place or not.

7. Second terms in the inner solutions

The existence of an induced slip velocity at the plate surface in D_0 means that is it necessary to proceed to another term in the inner series in order to see how this modifies the velocity and temperature profiles in D_i. Since the slip velocity has the value

$$\epsilon^{\frac{1}{2}}\psi_z^{(1)}(x > 0, 0) = \epsilon^{\frac{1}{2}}A(4x)^{-\frac{1}{4}}, \tag{42}$$

where A is defined in (39), it follows from matching that the stream function in D_i could be written in the form of (14) with

$$G_\psi^{(2)}(\epsilon) = \epsilon, \tag{43}$$

$$\Psi_Z^{(2)}(x, Z \to \infty) \to A(4x)^{-\frac{1}{4}} \tag{44}$$

(note the form of $\Psi^{(1)}$ in (17) and the final sentence in §4). Since p is now known to be of $O(\epsilon)$ in D_0 it can also be deduced that $\partial p/\partial x$ must be of this same order in D_i.

Now it is evident that re-writing terms such as $\rho u\,\partial u/\partial x$, for example, in the form $\rho u\,\partial[\rho u\theta]/\partial x$ by making use of (5) permits all of the conservation equations (1)–(4) to be expressed in terms of ψ [see equation (8)], θ and p alone. If an exact stretched stream function Ψ is defined so that

$$\psi = \epsilon^{\frac{1}{2}}\Psi, \tag{45}$$

these equations can be written in the inner domain D_i in the forms

$$\Psi_Z(\theta\Psi_Z)_x - \Psi_x(\theta\Psi_Z)_Z = (\mu(\theta\Psi_Z)_Z)_Z + 1 - \theta^{-1} + o(\epsilon^{\frac{1}{2}}), \tag{46}$$

$$\Psi_Z\theta_x - \Psi_x\theta_Z = Pr^{-1}(\lambda\theta_Z)_Z + o(\epsilon^{\frac{1}{2}}), \tag{47}$$

plus the result that p is constant up to and including terms of $O(\epsilon^{\frac{1}{2}})$. The error estimates in (46) and (47), and in the result for p, make use of the information which has been culled so far from the analysis, and the system now permits quick progress to the desired second approximations in D_i without the sacrifice of any accuracy in the representation of a variable-property system. This comes about because it is possible to define a new, 'exact', Howarth–Dorodnitsyn type of normal co-ordinate $\mathscr{Y}$ such that

$$\mathscr{Y} = \int_0^Z \frac{ds}{\theta(x, s)}, \tag{48}$$

and in terms of which (46) and (47) become

$$\Psi_{\mathscr{Y}}\Psi_{x\mathscr{Y}} - \Psi_x\Psi_{\mathscr{Y}\mathscr{Y}} = C\Psi_{\mathscr{Y}\mathscr{Y}\mathscr{Y}} + \theta - 1 + o(\epsilon^{\frac{1}{2}}), \tag{49}$$

$$\Psi_{\mathscr{Y}}\theta_x - \Psi_x\theta_{\mathscr{Y}} = (C/Pr)\theta_{\mathscr{Y}\mathscr{Y}} + o(\epsilon^{\frac{1}{2}}). \tag{50}$$

The quotients μ/θ and λ/θ which appear on the right-hand sides of the transformed equations in x, $\mathscr{Y}$ co-ordinates are of course equal to $\rho\mu$ and $\rho\lambda$, and these have been given the constant value C in accordance with the work in §4.

Appropriate forms for the inner series to second order are

$$\Psi(x, z:\epsilon) \sim \Psi^{(1)}(x, \mathscr{Y}) + \epsilon^{\frac{1}{2}}\Psi^{(2)}(x, \mathscr{Y}), \tag{51}$$

$$\theta(x, z:\epsilon) \sim \Theta^{(1)}(x, \mathscr{Y}) + \epsilon^{\frac{1}{2}}\Theta^{(2)}(x, \mathscr{Y}), \tag{52}$$

and it readily transpires that the solutions for $\Psi^{(1)}$ and $\Theta^{(1)}$ as functions of x and $\mathscr{Y}$, rather than of x and Y, follow at once from the previous results by writing $\mathscr{Y}$ in place of Y. If θ in (48) is given the value $\Theta^{(1)}$ then $\mathscr{Y}$ and Y are identical, since $R^{(1)}\Theta^{(1)}$ is equal to one; in view of (52), $\mathscr{Y}$ and Y will not generally remain equal to second order and $\Theta^{(2)}$ and $\Psi^{(2)}$ must now be found.

There is no need to write out the partial differential equations and boundary conditions for $\Psi^{(2)}$ and $\Theta^{(2)}$ in full; suffice it to say that they are linear equations with coefficients which depend on $\Psi^{(1)}$ and $\Theta^{(1)}$ and are such that, in the present case of the semi-infinite flat plate, the similitudes

$$\Psi^{(2)}(x, \mathscr{Y}) = C^{\frac{1}{2}}F^{(2)}(\eta), \tag{53}$$

$$\Theta^{(2)}(x, \mathscr{Y}) = (4x)^{-\frac{3}{4}}H^{(2)}(\eta) \tag{54}$$

exist, where η here is exactly the same as η in (19) except that Y is replaced by $\mathscr{Y}$.

Substitution of the solutions for $\Psi^{(1)}(x, \mathscr{Y})$ and $\Theta^{(1)}(x, \mathscr{Y})$ into the equation for $\Theta^{(2)}$, together with use of (43) and (54), shows that the ordinary differential equation for $H^{(2)}$ is homogeneous with homogeneous boundary conditions and that, in consequence,

$$H^{(2)}(\eta) \equiv 0 \equiv \Theta^{(2)}(x, \mathscr{Y}). \tag{55}$$

Thus the first-order result for θ in the inner domain is actually correct to within an error which is certainly $o(\epsilon^{\frac{1}{2}})$ for the semi-infinite flat plate, and this fact has already been noted by Yang & Jerger in their investigation of the finite-length-plate problem. Of course these authors go on to evaluate the effects of finiteness of the plate's chord (all for the case $M = 0$) and a brief word about their work is necessary here. Yang & Jerger assume (i) that the density is constant everywhere except in the term $1-\rho$ on the right-hand side of (2) (this is the familiar approximation in natural-convection theory which has already been referred to in the introduction), (ii) that the induced inflow which is represented by the boundary-value $\psi^{(1)}(x > 0, 0)$ in (35) actually applies only along the plate chord itself, so that (35) becomes, in the present notation,

$$\psi^{(1)}(0 < x < 1, 0) = \Delta^{\frac{1}{4}}(4x)^{\frac{3}{4}}F(\infty),$$
$$\psi^{(1)}(1 < x, 0) = 0,$$

where the plate is presumed to be of unit chord, and finally, (iii) that the fluid properties such as μ are evaluated at the reference temperature given by Sparrow & Gregg (1958).

Assumption (ii) follows from the speculation that there will be no inflow into the hot wake which exists above the plate and leads to an incompressible outer-domain flow which has a complex-conjugate velocity with singular behaviour (like $\ln[1-\zeta^{\frac{1}{4}}]$) as $\zeta = x+iz \to 1$. Their technique for solving the problem is to expand $u^{(1)}(0 < x < 1, 0)$ as a power series in $x^{m+\frac{1}{4}}$ ($m = 0, 1, 2, \ldots$) plus a term in $x^{-\frac{1}{4}}$ (which is actually the result for a semi-infinite plate) and thence to compute

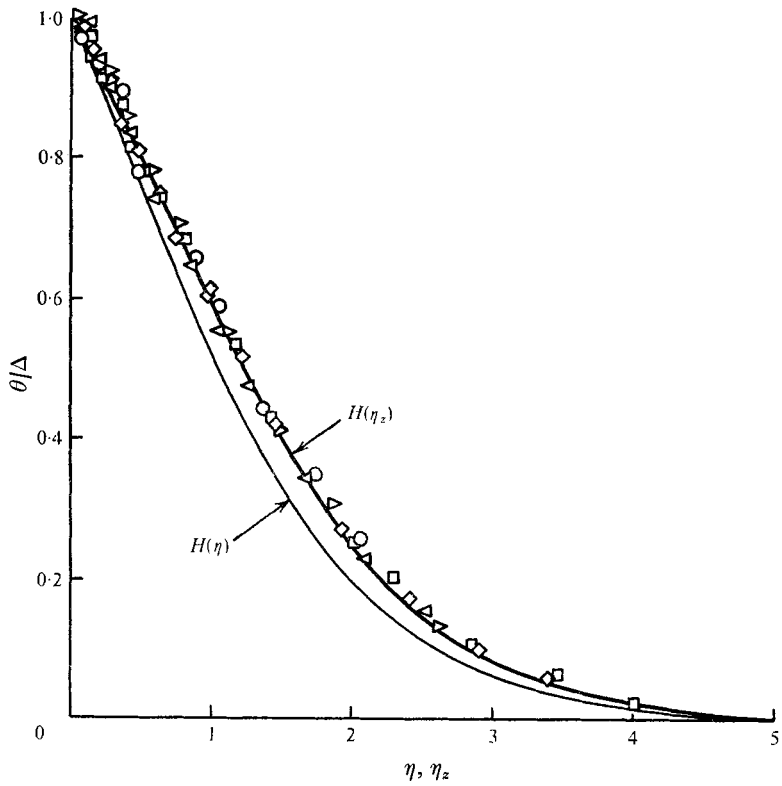

FIGURE 6. Comparison of the measured temperature profiles on a finite flat plate (Schmidt & Beckman) with the present theoretical results for a semi-infinite plate for zero blowing, namely $H(\eta_z)$; η_z is defined in (57). $H(\eta)$ is the solution uncorrected for the 'Howarth-stretching' and is the one given by Ostrach, for example. Experimental points: ○, $x = \frac{1}{12}$; □, $x = \frac{1}{6}$; ◇, $x = \frac{1}{3}$; ◁, $x = \frac{7}{12}$; ▷, $x = \frac{11}{12}$.

what we have written as $\Psi^{(2)}$ and $(4x)^{\frac{1}{4}}\Theta^{(2)}$ as series in $x^{m+\frac{1}{4}}$ with coefficients which are functions of a similarity variable like η. Yang & Jerger's comparisons of their results with the profile (temperature and velocity) measurements of Schmidt & Beckman (1930) are generally favourable, but it is necessary to make several observations about their theory.

First the result of assumptions (i) and (ii) above is that the similarity co-ordinate used by Yang & Jerger is, in present notation, equal to

$$\epsilon_{\mathrm{ref}}^{-\frac{1}{2}}\Delta^{\frac{1}{4}}z/(4x)^{\frac{1}{4}}, \tag{56}$$

where ϵ_{ref} is ϵ in (7) with ρ_0 and μ_0 replaced by their values at Sparrow & Gregg's reference temperature (i.e. $T_0'[1+0{\cdot}62\Delta]$ in present notation). Now the correct similarity co-ordinate in terms of the normal co-ordinate z, which we shall write as η_z, follows most readily from (48), (52) and (55), etc., in the form

$$\eta_z = \frac{\epsilon^{-\frac{1}{2}}z\Delta^{\frac{1}{4}}}{C^{\frac{1}{2}}(4x)^{\frac{1}{4}}} = \eta + \Delta\int_0^{\eta} H(s)\,ds + o(\epsilon^{\frac{1}{2}}), \tag{57}$$

where η is as given in (19) since Y and $\mathscr{Y}$ are synonymous to the order of accuracy

quoted when the plate is semi-infinite. When the dimensionless temperature difference in D_i, which is now known to be $H(\eta)+o(\epsilon^{\frac{1}{2}})$, is plotted against η_z (with C equal to one) and compared with the experimental results of Schmidt & Beckman for $M = 0$ it can be seen from figure 6 that the present theoretical results for a semi-infinite plate are at least as good as, if not slightly better than, Yang & Jerger's theory for a finite flat plate.

One must admit that the generalized Howarth–Dorodnitsyn transformation gives a more accurate representation of the dependence on the normal co-ordinate of a quantity like θ than can be achieved by use of a reference-temperature co-ordinate as in expression (56), if for no other reason than the fact that a result equivalent to (56) was arrived at by Sparrow & Gregg by making ϵ_{ref} the 'best-choice' average for the evaluation of overall quantities such as heat-transfer rate using a theory for gases based on the Howarth-type of transformation. These last-mentioned authors confined their attention to overall properties and did not use the Howarth transformation in comparisons of detailed temperature and velocity profiles; they were also interested only in the first inner solutions and hence in the co-ordinate Y. The extension of the present theory into the co-ordinate system $(x, \mathscr{Y})$ is not trivial, since it serves to indicate the high order of accuracy with which Y can represent dependence on the normal co-ordinate in D_i. One can now make use of this information to assess behaviour of the second approximation to the velocity component u in this same domain.

The exact result shows that velocity component u is equal to $\Psi_{\mathscr{Y}}$, whence the two-term inner series (51), together with (17) for $\Psi^{(1)}$ and (53) for $\Psi^{(2)}$, shows that

$$\frac{u}{(4x\Delta)^{\frac{1}{2}}} \sim F'(\eta)+\frac{\epsilon^{\frac{1}{2}}}{(4x)^{\frac{3}{4}}\Delta^{\frac{1}{4}}}F^{(2)\prime}(\eta). \tag{58}$$

With result (55) the equation satisfied by $F^{(2)}$ is found to be

$$F^{(2)\prime\prime\prime}+3FF^{(2)\prime\prime}-F'F^{(2)\prime} = 0 \tag{59a}$$

and the boundary conditions are [note, particularly, equation (44)] given by

$$F^{(2)}(0) = 0 = F^{(2)\prime}(0); \quad F^{(2)}(\eta\to\infty)\to 3C^{\frac{1}{2}}F(\infty). \tag{59b}$$

If $F^{(2)}(\eta)$ is written as $3C^{\frac{1}{2}}F(\infty)f_{00}(\eta)$, the function $f_{00}(\eta)$ is precisely the one already calculated by Yang & Jerger and so the solution for u in (58), for example, is complete for the case $M = 0$.

Apart from the present interpretations of ϵ and η in terms of physical co-ordinates and quantities, (58) is precisely the limit of Yang & Jerger's results for a semi-infinite flat plate and as such represents nothing new. However, as we have already seen with the temperature, the proper interpretations of ϵ and η are significant when comparisons with the experimental results of Schmidt & Beckman are made. The combination of (57) and (58) (with C given the value unity) is used to draw the curves in figures 7 (*a*)–(*e*) and, consulting Yang & Jerger's paper, it can be seen once again that the present results for the *semi-infinite* plate are at least as good as the results for the *finite* plate at reproducing the measurements. Figures 7 (*d*) and (*e*) do suggest that there may be some effect due to the wake, since the second-order theory for a semi-infinite plate is apparently not so good on

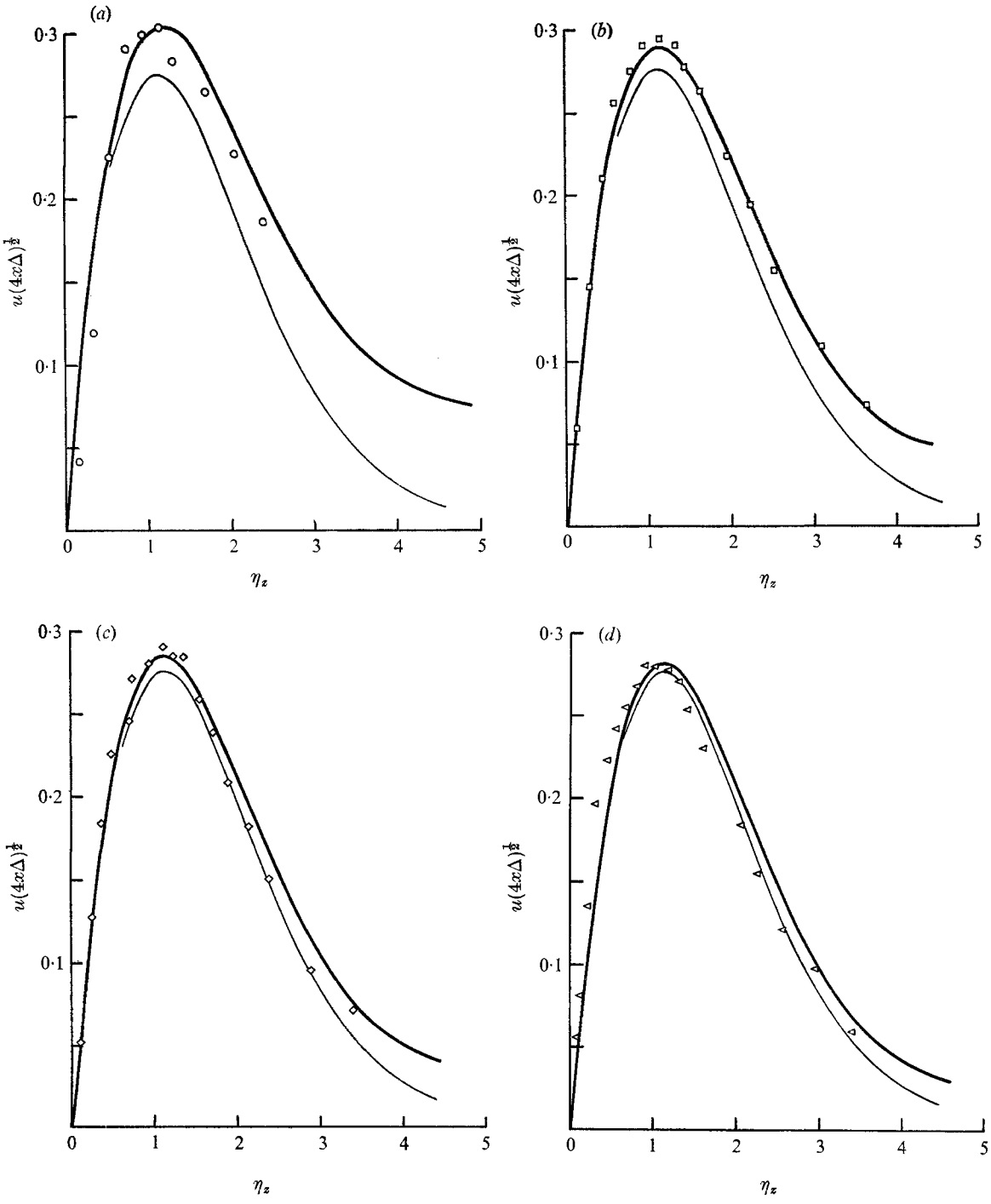

FIGURE 7. Comparison of the measured velocity profiles (open symbols) on a flat plate of unit chord (Schmidt & Beckman) at five chordwise stations with the present theoretical results (curves) for a semi-infinite plate for zero blowing; η_z is defined in (57). —, one term; —, two terms. (*a*) $x = \frac{1}{12}$, (*b*) $x = \frac{1}{6}$, (*c*) $x = \frac{1}{3}$, (*d*) $x = \frac{7}{12}$, (*e*) $x = \frac{11}{12}$.

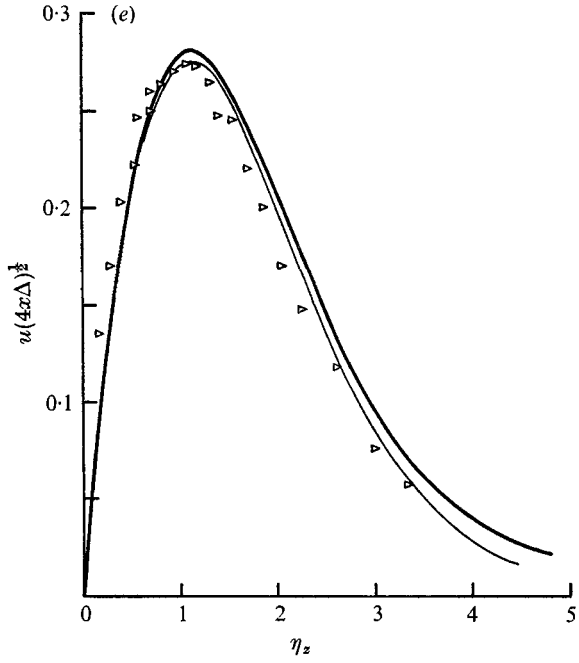

FIGURE 7(*e*). For legend see facing page.

the downstream half of the surface, but then the same is true of the theory for a finite flat plate. With great respect for the pioneering work of Yang & Jerger on the problem of a finite flat plate one must be tempted at this time to bring in a verdict of 'not proven'.

If the present theory is used for comparisons with measurements when M exceeds zero, then the contribution to η_z in (57) which comes from the integral of $H(\eta)$ will, as can be appreciated from figure 3, prove to be very large indeed.

The writer is greatly indebted to Dr James Eninger, TRW Systems, Redondo Beach, California, who very kindly supplied him with the numerical data for figures 2, 3 and 4.

REFERENCES

EDE, A. J. 1967 Advances in free convection. In *Advances in Heat Transfer*, vol. 4 (ed. J. P. Hartnett & T. F. Irvine). Academic.

EICHHORN, R. 1960 *Trans. A.S.M.E.* **82**, 260–263.

MERKIN, J. H. 1972 *Int. J. Heat Mass Transfer*, **15**, 989–999.

NACHTSHEIM, P. R. & SWIGERT, P. 1965 *N.A.S.A. Tech Note*, D-3004.

OSTRACH, S. 1964 Laminar flows with body forces. In *High Speed Aerodynamics and Jet Propulsion* (ed. F. K. Moore), vol. 4, *Theory of Laminar Flows*, §F. Oxford University Press. (See also 1953 *N.A.C.A. Rep.* no. 1111.)

RUPPERT, P. E. & LANDAHL, M. T. 1967 *Phys. Fluids*, **10**, 831–835.

SCHMIDT, E. & BECKMAN, W. 1930 *Tech. Mech. u. Thermodynamik*, **1**, 341–349, 391–406.

SPARROW, E. M. & CESS, R. D. 1961 *Trans. A.S.M.E.* **83**, 387–389.

SPARROW, E. M. & GREGG, J. L. 1958 *Trans. A.S.M.E.* **80**, 879–886.

YANG, K.-T. & JERGER, E. W. 1964 *J. Heat Transfer*, **86**, 107–115.